PHYSICAL REVIEW A **72**, 011801(R) (2005)

Three-photon-absorption resonance for all-optical atomic clocks

Sergei Zibrov,[1,2,3,4] Irina Novikova,[4] David F. Phillips,[4] Aleksei V. Taichenachev,[5] Valeriy I. Yudin,[5] Ronald L. Walsworth,[1,4] and Alexander S. Zibrov[1,3,4]

[1]*Department of Physics, Harvard University, Cambridge, Massachusetts 02138, USA*
[2]*Moscow State Engineering Physics Institute, Moscow 115409, Russia*
[3]*Lebedev Institute of Physics, Moscow 117924, Russia*
[4]*Harvard-Smithsonian Center for Astrophysics, Cambridge, Massachusetts 02138, USA*
[5]*Institute of Laser Physics SB RAS and Novosibirsk State University, Novosibirsk 630090, Russia*

(Received 18 January 2005; published 7 July 2005)

We report an experimental study of an all-optical three-photon-absorption resonance (known as an "*N* resonance") and discuss its potential application as an alternative to atomic clocks based on coherent population trapping. We present measurements of the *N*-resonance contrast, width and light shift for the D_1 line of ^{87}Rb with varying buffer gases, and find good agreement with an analytical model of this resonance. The results suggest that *N* resonances are promising for atomic clock applications.

DOI: 10.1103/PhysRevA.72.011801 PACS number(s): 42.72.−g, 42.50.Gy

There is great current interest in developing compact, robust atomic clocks with low power consumption and fractional frequency stability better than 10^{-12} for a wide variety of applications. In recent years, significant progress toward this goal has been achieved using coherent population trapping (CPT) resonances in atomic vapor [1–4]. In this paper, we investigate an all-optical three-photon-absorption resonance in Rb vapor [5], known as an "*N* resonance," which combines advantages of CPT and traditional optically pumped double resonance. We find that the *N* resonance provides high contrast with modest systematic frequency shifts, and thus may be suitable for small, stable atomic clocks.

An *N* resonance is a three-photon, two-field resonance, as shown in Fig. 1(a). An optical probe field, Ω_P, resonant with the transition between the higher-energy hyperfine level of the ground electronic state ($|b\rangle$) and an excited state ($|a\rangle$), optically pumps the atoms into the lower hyperfine level ($|c\rangle$), leading to increased transmission of the probe field through the medium. A second, off-resonant optical drive field, Ω_D, is detuned to lower frequencies than the $|b\rangle \rightarrow |a\rangle$ transition. If the difference frequency between Ω_P and Ω_D is equal to the hyperfine frequency, a two-photon resonance is created, driving atoms coherently from state $|c\rangle$ to $|b\rangle$, followed by a one-photon absorption from field Ω_P, which drives the atoms to the excited state $|a\rangle$ [6]. Thus, the absorption spectrum of the Ω_P field will have two distinct features [Fig. 1(a), bottom row]: a broad Doppler background due to linear absorption and a narrow resonance because of the three-photon nonlinear process. Importantly for clock applications, the *N* resonance is all optical.

For comparison, we also plot in Fig. 1 typical level diagrams and schematic spectra of the probe light transmission for CPT and traditional optically pumped double-resonance schemes. CPT is a two-photon transmission resonance [Fig. 1(b)] in which a coherence between two hyperfine levels is created by two resonant fields (Ω_P and Ω_D) whose frequency difference is equal to the hyperfine frequency. The absorption for both optical fields decreases due to destructive interference of the absorption amplitudes and a narrow transmission peak is observed. Several groups [2,3] have achieved fractional hyperfine frequency stabilities below 10^{-12} with CPT-based clocks, which are also promising for miniaturization. In the traditional optically pumped double-resonance clock [Fig. 1(c)], one optical field (from a lamp or laser diode) is resonant with one of the allowed transitions ($|b\rangle \rightarrow |a\rangle$), and thus optically pumps atoms to the other hyperfine sublevel ($|c\rangle$). A microwave field resonant with the ground-state hyperfine transition is applied, thereby redistributing the populations between the hyperfine levels and leading to a narrow dip in the transmission spectrum of the optical field. The width of this absorption feature is determined by the intensities of both the optical and microwave fields as well as the atoms' hyperfine decoherence rate. With careful optimization of operational parameters, short-term fractional stabilities of 10^{-11} may be achieved [7].

In practice, the frequency stability of an atomic clock lim-

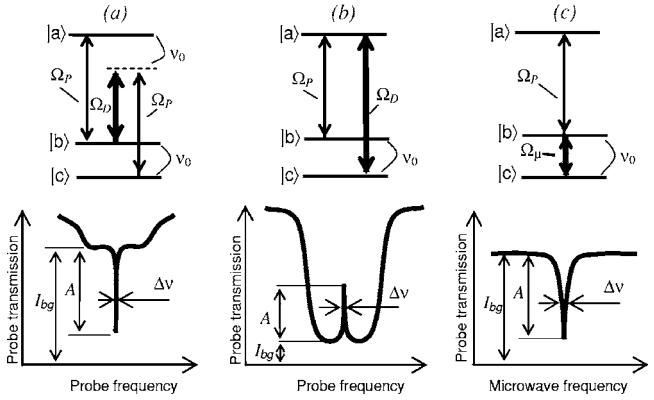

FIG. 1. Level diagrams (top row) and schematic representations of probe light transmission spectra for (a) *N* resonance, (b) CPT resonance, and (c) optical-pumping double-resonance schemes. Shown in the level diagrams are the relevant probe (Ω_P), drive (Ω_D), and microwave (Ω_μ) fields, as well as the ground-state hyperfine splitting ν_0. Shown in the schematic spectra are the full width ($\Delta\nu$) and relative intensity (A) of the clock resonance, and the intensity of the background transmitted light (I_{bg}).

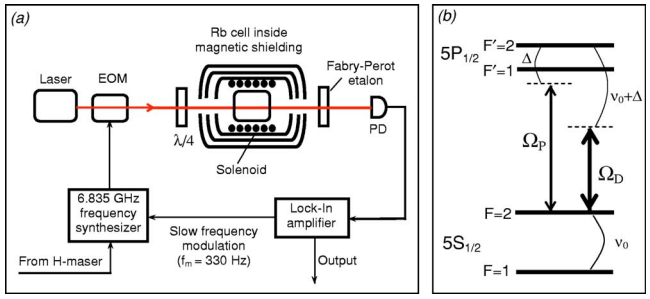

FIG. 2. (Color online) (a) Experimental apparatus. (b) Energy levels and applied fields (Ω_P, Ω_D) for N resonances on the D_1 line of ^{87}Rb. ν_0 is the ground electronic state hyperfine splitting and Δ is the detuning of the probe field from the $F=2 \rightarrow F'=2$ transition.

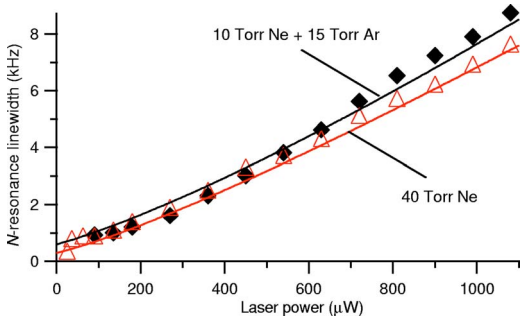

FIG. 3. (Color online) Measured N-resonance linewidth as a function of total incident laser power for ^{87}Rb vapor cells filled with 40 Torr of Ne buffer gas (Δ) and a mixture of 10-Torr Ne and 15 -Torr Ar (♦). The probe field is tuned ≈300 MHz below the $F=2 \rightarrow F'=2$ transition of ^{87}Rb. The solid lines are calculated linewidths using an analytical N-resonance model.

ited by photon shot noise is given by the Allan deviation, $\sigma(\tau)$, as [4]

$$\sigma(\tau) = \frac{1}{4}\sqrt{\frac{\eta e}{I_{bg}}}\frac{1}{\nu_0}\frac{\Delta\nu}{C}\tau^{-1/2}, \tag{1}$$

where ν_0 is the atomic reference frequency, $\Delta\nu$ is the full width of the resonance, e is the electron charge, η is the photodetector sensitivity (measured optical energy per photoelectron) and τ is the integration time. The resonance contrast $C \equiv A/I_{bg}$, where A is the relative intensity of the clock resonance and I_{bg} is the intensity of the background transmitted light (adopting notation similar to Ref. [4]). These contrast parameters are shown graphically in Fig. 1 for the N resonance, CPT resonance, and optically pumped double-resonance schemes.

Figure 2(a) shows a schematic of our N-resonance experimental setup. We derived the probe and drive optical fields (Ω_P and Ω_D) by phase modulating the output of an external cavity diode laser (≈12 mW total power) tuned in the vicinity of the D_1 line of Rb $(5^2S_{1/2} \rightarrow 5^2P_{1/2}, \lambda \simeq 795$ nm). An electro-optic modulator (EOM) produced the phase modulation of the optical field at a frequency near the ground electronic state hyperfine frequency of ^{87}Rb ($\nu_0 \simeq 6.835$ GHz). Approximately 2% of the incident laser power was transferred to each first-order sideband, with the remainder residing in the carrier. The laser beam was then circularly polarized using a quarter-wave plate and weakly focused to a diameter of 0.8 mm before entering the Rb vapor cell.

We employed Pyrex cylindrical cells containing isotopically enriched ^{87}Rb and either a 40-Torr Ne buffer gas or a 10-Torr Ne+15-Torr Ar mixture. During experiments, the vapor cell under study was heated to 55 °C using a blown-air oven. The cell was isolated from external magnetic fields with three layers of high permeability shielding. A small (≈10 mG) longitudinal magnetic field was applied to lift the degeneracy of the Zeeman sublevels and separate the desired $F=1$, $m_F=0$ to $F=2$, $m_F=0$ clock transition (no first-order magnetic field dependence) from the $m_F=\pm 1$ transitions (first-order Zeeman splitting).

To produce the N resonance we tuned the high frequency optical sideband (serving as the probe field Ω_P) near resonance with the $5S_{1/2}$ $F=2 \rightarrow 5P_{1/2}$ $F'=1,2$ transitions. The strong laser carrier field at a frequency 6.835 GHz below this transition was used as the drive field Ω_D [see Fig. 1(a)]. Note that we operate in the regime of relatively low laser power and atomic density, which is different from [5]. In the present case all four-wave mixing processes are insignificant, and the far-off-resonance lower frequency sideband had negligible effect on the atoms. The strong drive field and the lower sideband were filtered from the light transmitted through the cell using a quartz, narrow-band Fabry-Perot etalon (FSR =20 GHz (where FSR is free spectral range), finesse=30), tuned to the frequency of the probe field and placed before the photodetector. Such selective detection reduces the light background (I_{bg}) by eliminating nonreasonant leakage from the drive field; and also increases the absorption amplitude (A) by eliminating the stimulated Raman drive field created at two-photon resonance [5]. Our analytical modeling of the N resonance—based on the method developed in [8,9] for CPT resonances—indicates that the absorption amplitude A increases by ≈1.7 when only the probe field transmission is detected. (Details of this analytical model will be described in a future publication.)

Figure 3 shows measured N-resonance linewidths for two different buffer gases. At lower laser power, linewidths <1 kHz are observed: e.g., $\Delta\nu \approx 300$ Hz at 50 μW total laser power for the 40-Torr Ne cell. At larger laser powers the linewidth increases approximately linearly with laser power. As also shown in Fig. 3, our calculations are in good agreement with the measured variation of linewidth with laser power.

Figure 4 shows measurements of the N-resonance contrast $C=A/I_{bg}$ for two buffer gas cells. For both cells the contrast increases rapidly with laser power, and then saturates at $C>15\%$ for total incident laser power ~1 mW due to optical pumping to other Zeeman sublevels. (The background transmission is 50–90 %, depending on the laser power.) This saturated N-resonance contrast exceeds the contrast that has been achieved to date with traditional CPT clock resonances, $C<4\%$ [4]. However, the relatively large laser power required to saturate the N-resonance contrast leads to an increased linewidth (see Fig. 3). To account for these competing effects of laser power, we follow Vanier *et al.* [4] and employ a resonance quality factor $q \equiv C/\Delta\nu$ as a figure

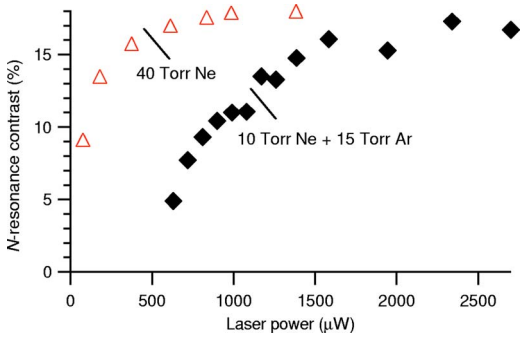

FIG. 4. (Color online) Measured dependence of N-resonance contrast on the total incident laser power for two buffer gas cells: 40-Torr Ne (Δ) and 10-Torr Ne+15-Torr Ar (♦). The probe field is tuned ≈300 MHz below the $F=2\rightarrow F'=2$ transition of ^{87}Rb.

of merit for N-resonance clocks. For example, for 120 μW of laser power for the 40-Torr Ne cell, we find $\Delta\nu\approx 1$ kHz and $C\approx 0.1$ for the ^{87}Rb N resonance (see Figs. 3 and 4), implying $q\approx 10^{-4}$ and an estimated frequency stability from Eq. (1) of $\sigma(\tau)\sim 10^{-14}\tau^{1/2}$.

Importantly, Fig. 4 also shows that the N-resonance contrast reaches its maximum at lower laser powers for the higher-pressure 40-Torr Ne vapor cell than for the cell with the 25-Torr Ne-Ar mixture. We attribute this difference to slower Rb diffusion out of the laser fields at higher buffer gas pressure, and hence reduced ground-state coherence loss and more efficient optical pumping. In addition, we did not observe a deterioration of the N-resonance contrast with increased buffer gas pressure, as has been observed for CPT resonances [4]. This observation suggests that the N resonance may be a good candidate for miniature atomic clocks, where high buffer gas pressure is required to prevent rapid atomic decoherence due to collisions with the walls of a small vapor cell.

We also characterized the light shift of the ^{87}Rb N resonance. A light shift is a relative ac Stark shift of atomic levels that depends on both the optical field frequency and intensity [10]. Light shifts are a primary systematic effect limiting the frequency stability of optically pumped atomic clocks. To leading order in a simple picture that includes the near resonant effects of the probe field, the light shift, Δ_{ls}, of the clock frequency is given by

$$\Delta_{ls} = -\frac{\Delta}{\gamma_{ab}^2 + 4\Delta^2}|\Omega_P|^2, \qquad (2)$$

where Δ is the detuning of the probe field. For small Δ, the light shift is linear in the laser frequency (Δ) and intensity ($\propto|\Omega_P|^2$). Fluctuations in these parameters are thus directly transferred to the clock frequency. For example, light shifts limit the fractional frequency stability of optically pumped double-resonance clocks at the level of 10^{-11} [11–13].

In practice, the diode laser typically used in a CPT clock is driven with strong current modulation to produce the two strong, resonant optical fields Ω_P and Ω_D. This modulation scheme necessarily leads to: (i) higher-order sidebands, which, even when optimally adjusted, can induce nontrivial second-order light shifts [4,14]; and (ii) unwanted

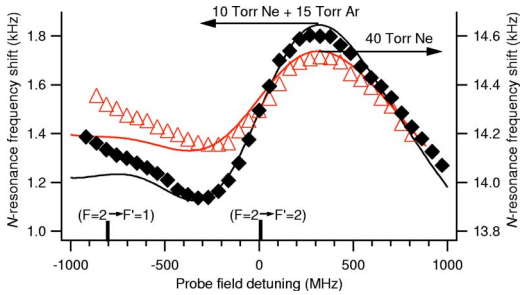

FIG. 5. (Color online) Measured variation of the N-resonance frequency as a function of probe field detuning from the ^{87}Rb $F=2\rightarrow F'=2$ transition with total incident laser power of 450 μW. Right vertical axis: 40-Torr Ne (Δ). Left vertical axis: 25-Torr Ne-Ar mixture (♦). These N-resonance frequencies include a buffer gas pressure shift of the ^{87}Rb ground-state hyperfine frequency: about 14 kHz for the 40-Torr Ne cell and 1 kHz for the 25-Torr Ne-Ar mixture [15,16]. The solid lines are calculations from an analytical model.

amplitude modulation of the optical fields, resulting in an imbalance between sideband intensities as large as 10% [2]. These imperfections lead to residual light shifts of ~0.2 Hz/(μW/cm^2) (for shifts induced by changes in the carrier field intensity) and ~1–10 mHz/MHz (for shifts induced by changes in the carrier field frequency) [2–4]. In practice, the short- and medium-term frequency stability of CPT clocks is limited by such light shifts [3,4].

As shown in Fig. 5, we measured two extrema in the N-resonance light-shift as a function of probe field frequency. At these extrema the light shift depends quadratically on the probe field detuning. Additionally, the second-order light shift near the extrema is reduced at higher buffer gas pressure, from approximately 4.0 mHz/MHz^2 for the 25-Torr Ne-Ar mixture to 2.5 mHz/MHz^2 for the 40-Torr Ne cell, suggesting again that N resonances may be well suited to small vapor cells employing high buffer gas pressure. Figure 6 shows the measured dependence of the N-resonance light shift on total laser power. We find a linear dependence, with a similar variation of 25 mHz/(μW/cm^2)

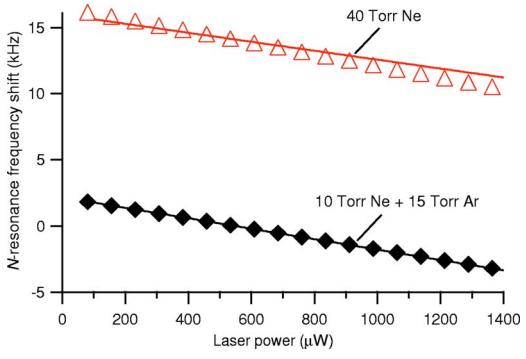

FIG. 6. (Color online) Measured dependence of the N-resonance frequency on the total incident laser power, with the probe field tuned ≈300 MHz below the $F=2\rightarrow F'=2$ transition of ^{87}Rb. Upper trace: 40-Torr Ne (Δ). Lower trace: 25-Torr Ne-Ar mixture (♦). As in Fig. 5, the N-resonance frequencies include the buffer gas pressure shift. The solid lines are calculations from an analytical model.

for different buffer gases. Moreover, our calculations indicate that the *N*-resonances light shifts may be reduced further with optimization of the microwave modulation index.

Finally, we note that *N* resonances on the D_2 line of alkali vapor may also be promising for clock applications. Our analytical model suggests higher *N*-resonance contrast on the D_2 transition due to strong collisional mixing of the Zeeman levels in the electronic excited state, which suppresses optical pumping to the end Zeeman levels in the ground electronic state. CPT contrast is smaller for the D_2 line than for the D_1 line due to pressure broadening of the excited state hyperfine levels [17]. Currently, diode lasers on the D_2 line of Rb and Cs are more easily obtained.

In summary, we measured the properties of an *N* resonance on the D_1 line in Rb vapor cells with varying buffer gases. We found that this *N* resonance has greater contrast and smaller light-shifts than the corresponding CPT resonance. These results suggest that an all-optical atomic clock locked to an *N* resonance may provide improved short and medium term frequency stability compared to CPT clocks. In addition, we found that the *N*-resonance contrast does not degrade, nor the light shifts worsen, with increased buffer gas pressure. Hence, *N* resonances may be good candidates for miniature atomic clocks.

The authors are grateful to M.D. Lukin, and V.L. Velichansky for useful discussions. This work was supported by DARPA. Work at the Center for Astrophysics was also supported by ONR and the Smithsonian Institution. A. V. T. and V. I. Y. acknowledge support from RFBR (Grants No. 05-02-17086 and 04-02-16488).

[1] N. Cyr, M. Têtu, and M. Breton, IEEE Trans. Instrum. Meas. **42**, 640 (1993).
[2] S. Knappe, R. Wynands, J. Kitching, H. G. Robinson, and L. Hollberg, J. Opt. Soc. Am. B **18**, 1545 (2001).
[3] M. Merimaa, T. Lindwall, I. Tittonen, and E. Ikonen, J. Opt. Soc. Am. B **20**, 273 (2003).
[4] J. Vanier, M. W. Levine, D. Janssen, and M. J. Delaney, IEEE Trans. Instrum. Meas. **52**, 822 (2003).
[5] A. S. Zibrov, C. Y. Ye, Y. V. Rostovtsev, A. B. Matsko, and M. O. Scully, Phys. Rev. A **65**, 043817 (2002).
[6] W. Happer and B. S. Mathur [Phys. Rev. Lett. **18**, 727 (1967)] observed such coherent population transfer with a modulated incoherent light source. Thus practical *N* resonances may be possible using a Rb lamp as the light source.
[7] J. Vanier and C. Audoin, *The Quantum Physics of Atomic Frequency Standards* (Hilger, New York, 1989).
[8] A. V. Taichenachev, V. I. Yudin, R. Wynands, M. Stahler, J. Kitching, and L. Hollberg, Phys. Rev. A **67**, 033810 (2003).
[9] S. Knappe, M. Stahler, C. Affolderbach, A. V. Taichenachev, V. I. Yudin, and R. Wynands, Appl. Phys. B **76**, 57 (2003).
[10] B. S. Mathur, H. Tang, and W. Happer, Phys. Rev. **171**, 11 (1968).
[11] L. A. Budkin, V. L. Velichanskii, A. S. Zibrov, A. A. Lyalyaskin, M. N. Penenkiov, and A. I. Pikhtelev, Sov. J. Quantum Electron. **20**, 301 (1990).
[12] J. C. Camparo and S. B. Delcamp, Opt. Commun. **120**, 257 (1995).
[13] G. Mileti, J. Deng, F. L. Walls, D. A. Jennings, and R. E. Drullinger, IEEE J. Quantum Electron. **34**, 233 (1998).
[14] M. Zhu and L. S. Cutler, in Proceedings of the 32nd Annual Precise Time and Time Interval (PTTI) Systems and Applications Meeting, 2000, edited byL.Breakiron (USNO, Washington, 2001), p. 311.
[15] M. Erhard and H. Helm, Phys. Rev. A **63**, 043813 (2001).
[16] Ch. Ottinger, R. Scheps, G. W. York, and A. Gallagher, Phys. Rev. A **11**, 1815 (1975).
[17] M. Stahler, R. Wynands, S. Knappe, J. Kitching, L. Hollberg, A. Taichenachev, and V. Yudin, Opt. Lett. **27**, 1472 (2002).